

# Contractions of Lie algebras and separation of variables. The $n$ -dimensional sphere

A. A. Izmet's'ev, G. S. Pogosyan, and A. N. Sissakian

*Joint Institute for Nuclear Research, Dubna, Moscow Region 141980, Russia*

P. Winternitz<sup>a)</sup>

*Centre de Recherches Mathématiques, Université de Montréal, C. P. 6128,  
succ. Centre Ville, Montréal, Québec H3C 3J7, Canada*

(Received 1 April 1998; accepted for publication 24 September 1998)

Inönü–Wigner contractions from the rotation group  $O(n+1)$  to the Euclidean group  $E(n)$  are used to relate the separation of variables in Laplace–Beltrami operators on  $n$ -dimensional spheres and Euclidean spaces, respectively. In this article we consider all subgroup type coordinates corresponding to different chains of subgroups of  $O(n+1)$  and  $E(n)$ , respectively. In particular, the contractions relate the graphical formalism of “trees” on spheres to the “clusters” on Euclidean spaces (introduced in this article). The contractions are considered analytically on several levels: the vector fields realizing the Lie algebras, the complete sets of commuting operators characterizing separable coordinate systems, the coordinate systems themselves and the separated eigenfunctions. © 1999 American Institute of Physics. [S0022-2488(99)04102-X]

## I. INTRODUCTION

Our purpose in this article is to use Lie algebra contractions to relate the separation of variables in Helmholtz equations on  $n$ -dimensional spheres  $S_n$  and on the Euclidean spaces  $E_n$ . An earlier article<sup>1</sup> was devoted to the case  $n=2$ . It was shown that spherical coordinates on  $S_2$  can be contracted either to polar or Cartesian ones on  $E_2$ . Elliptic coordinates on  $S_2$  were contracted to elliptic, parabolic and Cartesian ones on  $E_2$ .

The more complicated case of contractions from a two-dimensional Lorentzian hyperboloid  $H_2$  to  $E_2$  has also been studied.<sup>2</sup>

Here we are interested in the case of  $S_n$  for arbitrary  $n$ , but will only consider the simplest types of coordinates, the so-called subgroup type coordinates.<sup>3–8</sup> For  $S_n$  these are polyspherical coordinates introduced by Vilenkin<sup>9,10</sup> and described by the “method of trees.”<sup>9–13</sup> Trees, or “clusters” can, of course, also be introduced to describe subgroup type coordinates in  $E_n$ , and we shall show how “trees” on  $S_n$  are related to “clusters” on  $E_n$  via the group contraction  $O(n+1) \rightarrow E(n)$ .

At least two definitions of Lie algebra contractions exist in the literature. The original Inönü–Wigner contractions<sup>14–16</sup> can be viewed as singular changes of bases. The more recent “graded contractions”<sup>17–23</sup> are obtained as deformations of the original Lie algebra via modifications of the commutation relations, preserving a given grading of the Lie algebra. In many cases, though not all, the two concepts are equivalent.<sup>23</sup> In particular, the contractions considered in this article are simultaneously Inönü–Wigner and  $Z_2$ -graded ones.

Our main tool for dealing with contractions is the concept of “analytic contractions,” already introduced in Ref. 1. The generators of the original Lie algebra, in our case  $o(n+1)$ , are written as differential operators, involving the contraction parameters, in our case the radius  $R$  of the sphere. The parametrization must be such that in the contraction limit, in which the  $o(n+1)$

<sup>a)</sup>Electronic mail: WINTERN@CRM.UMONTREAL.CA

algebra contracts to the  $e(n)$  one, the generators themselves as differential operators, contract into generators of  $e(n)$ .

As a motivation for this study we mention, first of all, the theory of special functions. Indeed contractions relate two different groups and their homogeneous spaces. They relate separable coordinates in these two spaces, the separated equations and their solutions. The contractions will thus, in particular, provide asymptotic formulas and other relations between special functions.

Other applications concern the relations between integrable systems in different spaces, in particular, on spheres  $S_n$  and Euclidean spaces  $E_n$ . Indeed, each separable system can be extended by adding a potential that allows separation. The corresponding Hamiltonian systems will be integrable both on  $S_n$  and  $E_n$ , since they will also have  $n$  integrals of motion in involution. Again, the contractions relate the  $S_n$  and  $E_n$  integrable systems and their solutions.

In Sec. II we review some known results on the method of trees for  $S_n$ .<sup>9-13</sup> We introduce  $O(n)$  subgroup diagrams and relate them to the tree diagrams. Section III is devoted to the separation of variables in Euclidean spaces  $E_n$ . We introduce  $E(n)$  subgroup diagrams,  $E_n$  "cluster" diagrams, and relate the two. Beltrami coordinates are used in Sec. IV to introduce the radius of the sphere into the expressions for the elements of the  $o(n+1)$  Lie algebras. This provides the tools for an analytical realization of the Lie algebra contraction  $o(n+1) \rightarrow e(n)$ . The contraction of the coordinate systems and the complete sets of commuting operators is presented in Sec. V. Finally, the asymptotic formulas representing contractions of the solutions of the Laplace-Beltrami equation on  $S_n$  to those of the Helmholtz equation on  $E_n$  are presented in Sec. VI.

## II. SUBGROUP TYPE COORDINATES AND THE METHOD OF TREES

### A. Subgroups of Lie groups and separable coordinates

We shall make use of an algebraic approach to separating variables in Helmholtz (and Hamilton-Jacobi) equations in Riemannian and pseudo-Riemannian spaces that are homogeneous spaces for some Lie group  $G$ .<sup>3-8</sup>

The equation that we are interested in can be written as

$$\Delta_{LB}\Psi = E\Psi, \quad \Delta_{LB} = \frac{1}{\sqrt{g}} \frac{\partial}{\partial \xi^i} \sqrt{g} g^{ij} \frac{\partial}{\partial \xi^j}, \quad g = |\det g_{ij}|, \tag{2.1}$$

where  $g_{ij}$  is the metric tensor written in the considered coordinates  $\xi_i$ . The space  $M$  can be identified with some factor space  $M \sim G/G_0$ , where  $G_0$  is the isotropy group of the origin.

The separated solutions of Eq. (2.1) are simultaneous eigenfunctions of some complete set of  $n$  commuting operators  $Y_a$  (including the Laplace-Beltrami operator). We thus have

$$Y_a \Psi = \lambda_a \Psi, \quad \Psi = \prod_{i=1}^n \Psi_i(\zeta_i; \lambda_1, \lambda_2, \dots, \lambda_n). \tag{2.2}$$

The operators  $Y_a$  are second order operators in the enveloping algebra of the Lie algebra of the isometry group  $G$ . Thus we have a Lie algebra  $L$  with basis  $L \sim \{X_1, \dots, X_N\}$  and put

$$Y_a = A_{ik}^a X_i X_k, \quad [Y_a, Y_b] = 0, \quad A_{ik}^a = A_{ki}^a; \quad a = 1, 2, \dots, n. \tag{2.3}$$

The commuting sets of operators  $\{Y_1, \dots, Y_n\}$  can be classified into conjugacy classes under the action of the group  $G$ . Mutually conjugate sets provide equivalent systems of coordinates, transformed amongst each other by the group  $G$ .

A classification of the sets  $\{Y_a\}$  provides a classification of coordinate systems. The essential properties of the coordinate systems are related to properties of the operators  $Y_a$ . In particular, ignorable coordinates<sup>24</sup>  $\xi_j$  (i.e., coordinates that do not figure in the metric tensor  $g_{ik}$ ) are associated with operators  $Y_j$  that are squares of elements of the Lie algebra,

$$Y_j = \left\{ \sum_{k=1}^N a_{jk} X_k \right\}^2 = \frac{\partial^2}{\partial \alpha_j^2}. \tag{2.4}$$

Hence, maximal Abelian subalgebras<sup>25-31</sup> of the algebra  $L$  will provide maximal sets of ignorable variables.

Particularly simple coordinate systems are obtained if all operators  $Y_a$  in a given set are either squares of elements in the Lie algebra  $L$ , as in Eq. (2.4), or Casimir operators of subalgebras of  $L$ . Such coordinate systems have been called *subgroup type coordinates*.<sup>6</sup> Thus, consider a chain of subalgebras,

$$L \supset L_1 \supset L_2 \supset \dots \supset L_M, \tag{2.5}$$

such that each subalgebra  $L_j$  has at least one second order Casimir operator (second order operator in the center of the enveloping algebra of  $L_j$ ). Subgroup type coordinates are obtained if the chain of subalgebras provides  $n$  linearly independent second order operators. They will automatically commute amongst each other.

In this article we restrict our attention to subgroup type coordinates on spheres  $S_n$  and Euclidean spaces  $E_n$ . We mention that on  $S_2$  precisely two types of separable coordinates exist. Spherical coordinates are subgroup type, the subgroup chain being  $O(3) \supset O(2)$ . Elliptic coordinates are not of the subgroup type. On  $S_3$ , six separable coordinate systems exist,<sup>6,32,33</sup> two of them of the subgroup type, corresponding to the chain  $O(4) \supset O(3) \supset O(2)$  and  $O(4) \supset O(2) \otimes O(2)$ , respectively. For  $E_3$ , three out of eleven separable coordinate systems are of the subgroup type: Cartesian, cylindrical and spherical.

A graphical method, called the "method of trees," has been developed to treat subgroup type coordinates on real and complex spheres.<sup>9-13</sup> We will reproduce some of the relevant results for *real* spheres  $S_n$  in the following subsection, and then extend them to analyze subgroup type coordinates on  $E_n$ . Moreover, we will connect the tree diagrams with subgroup diagrams, introduced below.

**B. Subgroup type coordinates on  $S_n$  and the method of trees**

Let us consider the Lie algebra  $o(n+1)$  and use the standard basis of operators on  $S_n$ :

$$L_{ik} = (u_i \partial_k - u_k \partial_i);$$

$$[L_{ij}, L_{rs}] = -g_{js} L_{ir} - g_{ir} L_{js} + g_{jr} L_{is} + g_{is} L_{jr}, \quad 0 \leq i, k, j, r, s \leq n. \tag{2.6}$$

Let us now consider the defining representation of  $o(n+1)$  by matrices

$$X \in \mathcal{R}^{(n+1)(n+1)}, \quad X^T + X = 0, \tag{2.7}$$

acting on the space  $\mathcal{R}^{(n+1)}$ . Maximal reducibly imbedded subalgebras of  $o(n+1)$  will leave some vector subspace of  $\mathcal{R}^n$  invariant. All subalgebras of this type have the form

$$o(n+1) \supset o(n_1) \oplus o(n_2), \quad n_1 + n_2 = n + 1, \quad n_1 \geq n_2 \geq 2, \quad \text{or} \quad o(n+1) \supset o(n). \tag{2.8}$$

Maximal irreducibly imbedded subalgebras also exist, e.g.,  $u(n) \subset o(2n)$  or  $g_2 \subset o(7)$ , but they will not be needed here.

Chains of mutually maximally imbedded subalgebras are obtained by further splitting  $o(n_1)$  and  $o(n_2)$  into pairs of algebras, until we end the chain with one-dimensional subalgebras  $o(2)$  [we drop all the  $o(1) \sim \{0\}$  algebras]. We shall describe subalgebra chains by subalgebra diagrams (or equivalently subgroup diagrams). Each  $O(k)$  subgroup is represented by a circle with the corresponding number  $k$  in it. All subgroup diagrams of this type are shown in Fig. 1 for  $n \leq 5$ . Their recursive character is obvious: different subgroup diagrams for a given  $O(n)$  correspond to different flags of invariant subspaces of  $\mathcal{R}$ .


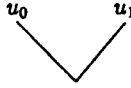

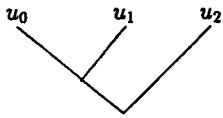

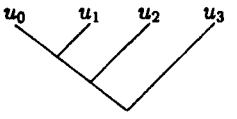
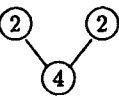
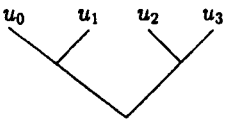

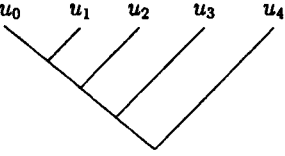
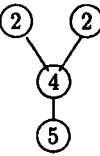
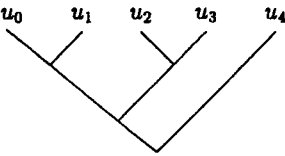
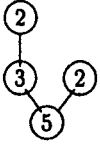
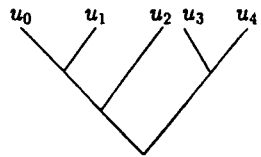
| No. | Subgroup chain                                | Subgroup diagram  | Tree diagram   |
|-----|---|---|--|
| 2   | $O(2)$  |    |     |
| 3   | $O(3) \supset O(2)$                           |    |    |
| 4.1 | $O(4) \supset O(3) \supset O(2)$              |    |    |
| 4.2 | $O(4) \supset O(2) \otimes O(2)$              |    |    |
| 5.1 | $O(5) \supset O(4) \supset O(3) \supset O(2)$ |    |    |
| 5.2 | $O(5) \supset O(4) \supset O(2) \otimes O(2)$ |   |   |
| 5.3 | $O(5) \supset O(3) \otimes O(2) \supset O(2)$ |  |  |

FIG. 1. Subgroup and tree diagrams for  $S_n$ .

The subgroup diagrams are closely related to the tree diagrams of Vilenkin,<sup>9,10</sup> describing polyspherical coordinates on  $S_n$ . In Fig. 1 we associate a tree diagram with each subgroup diagram for  $2 \leq n \leq 5$ . Families of different, but topologically equivalent, trees are associated with the same subgroup diagram. They are obtained either by permuting the end points, corresponding to the coordinates, or, equivalently, by rotating branches around branching points on the tree. All different trees, including equivalent ones, are shown for  $S_2, S_3, S_4$  in Fig. 2.

The tree diagrams are best described in the original article<sup>9</sup> and the book.<sup>13</sup> Together with the subgroup diagrams described above, they provide a tool for writing coordinates on  $S_n$ , complete sets of commuting operators and their eigenvalues and separated solutions of the Helmholtz equation.

Let us recall some basic facts here, using the example of a specific tree, namely that in Fig. 3 for  $S_7$ . In Fig. 3(a) we give the corresponding  $O(8)$  subgroup diagram. The actual  $S_7$  tree is in Fig. 3(b). Figures 3(c) and 3(d) refer to the  $E(7)$  group and  $E_7$  space (after contraction) and will be used below.

Each end point on the tree of Fig. 3(b) corresponds to a Cartesian coordinate in the ambient

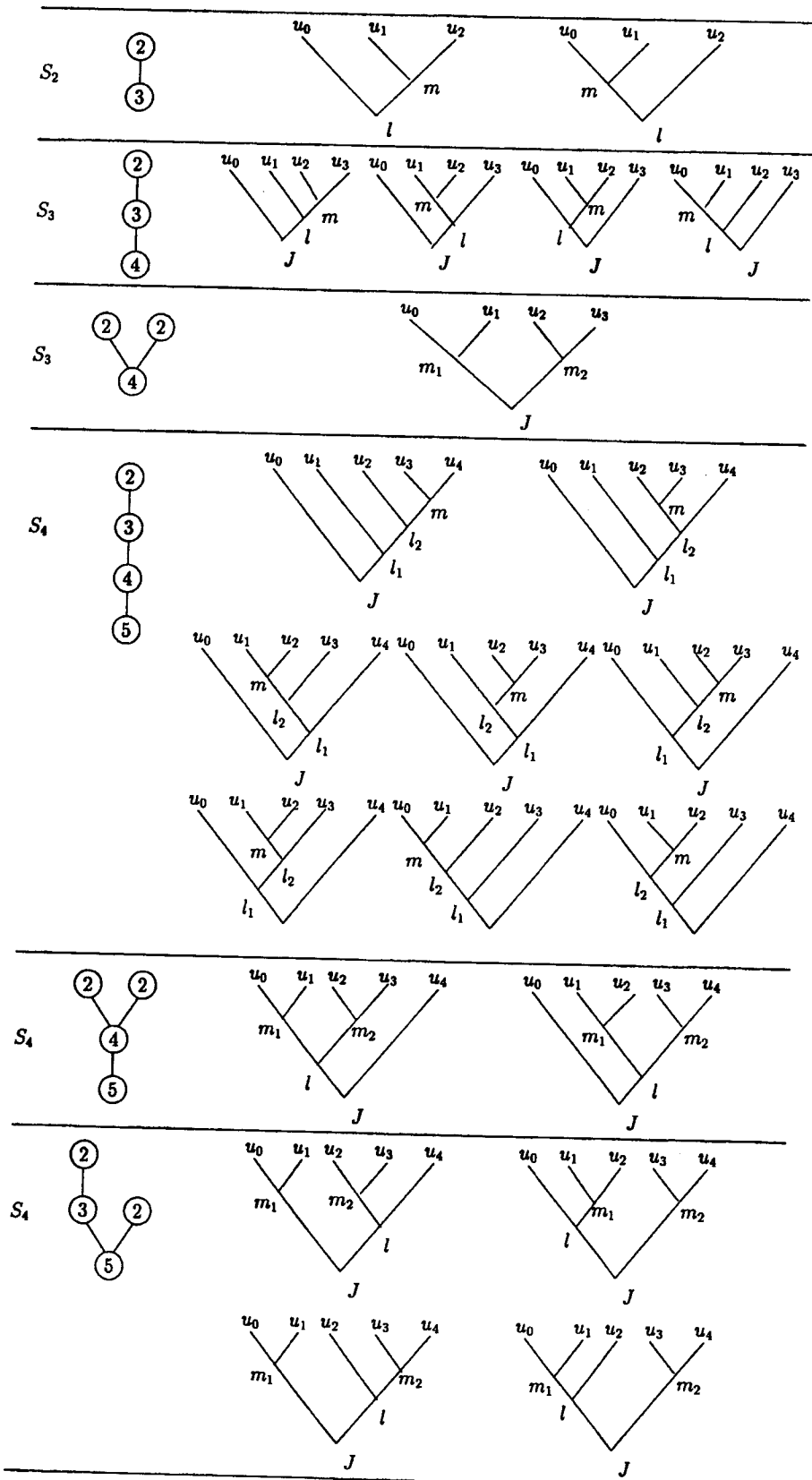


FIG. 2. Equivalent tree diagrams corresponding to one subgroup diagram for  $S_n$ .

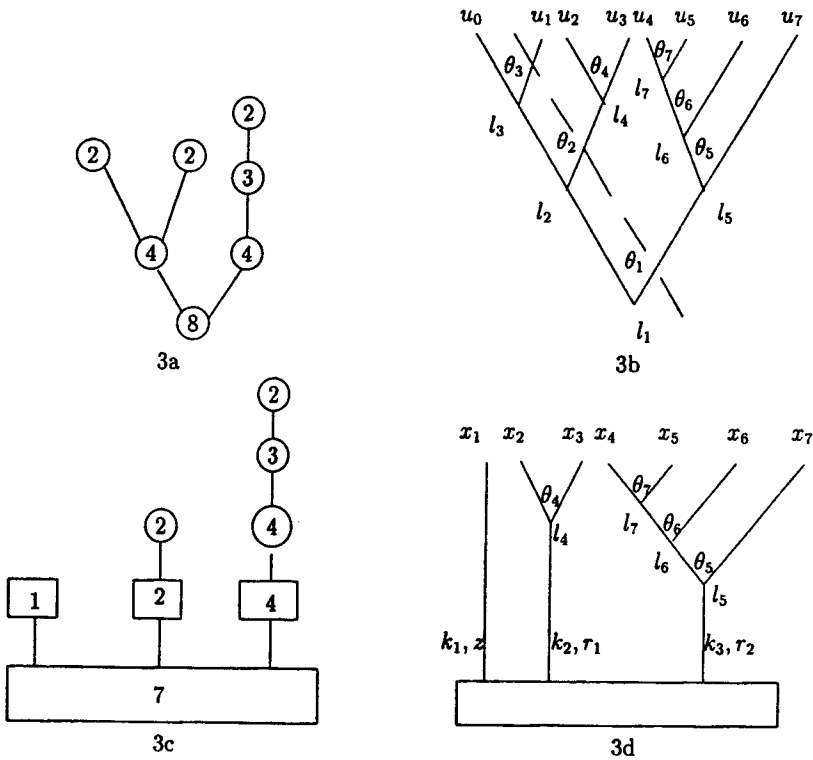


FIG. 3. Examples: An  $O(8)$  subgroup diagram (3a) and the corresponding  $S_7$  tree diagram (3b). An  $E(7)$  subgroup diagram (3c) and the corresponding  $E_7$  cluster diagram.

space  $\mathcal{R}^8$ . At each branching point we introduce an angle  $\theta_i$ . We move along the tree from the ground upwards to a specific coordinate  $u_i$ . At each branching point we write  $\cos \theta_a$  if we go to the left,  $\sin \theta_a$  if we go to the right. The polyspherical coordinates corresponding to Fig. 3(b) hence are

$$\begin{aligned}
 u_0 &= R \cos \theta_1 \cos \theta_2 \cos \theta_3, & u_4 &= R \sin \theta_1 \cos \theta_5 \cos \theta_6 \cos \theta_7, \\
 u_1 &= R \cos \theta_1 \cos \theta_2 \sin \theta_3, & u_5 &= R \sin \theta_1 \cos \theta_5 \cos \theta_6 \sin \theta_7, \\
 u_2 &= R \cos \theta_1 \sin \theta_2 \cos \theta_4, & u_6 &= R \sin \theta_1 \cos \theta_5 \sin \theta_6, \\
 u_3 &= R \cos \theta_1 \sin \theta_2 \sin \theta_4, & u_7 &= R \sin \theta_1 \sin \theta_5.
 \end{aligned}
 \tag{2.9}$$

The complete set of 7 commuting operators is also read off from the tree diagram, or from the subgroup one. We have

$$\begin{aligned}
 Y_3 &= L_{01}^2, & Y_4 &= L_{23}^2, & Y_7 &= L_{45}^2, & Y_6 &= L_{45}^2 + L_{56}^2 + L_{46}^2, \\
 Y_2 &= \sum_{0 \leq i < k \leq 3} L_{ik}^2, & Y_5 &= \sum_{4 \leq i < k \leq 7} L_{ik}^2, & Y_1 &= \sum_{0 \leq i < k \leq 7} L_{ik}^2.
 \end{aligned}
 \tag{2.10}$$

We see that  $Y_3, Y_4$  and  $Y_7$  are Casimir operators of  $o(2)$  algebras,  $Y_6$  of an  $o(3)$  one,  $Y_2$  and  $Y_5$  correspond to  $o(4)$  algebras and  $Y_1$  is the original  $o(8)$  Casimir operator. More generally, each ring in the subgroup chain provides the Casimir operator of the corresponding  $o(k)$  to the set  $\{Y_a\}$ .

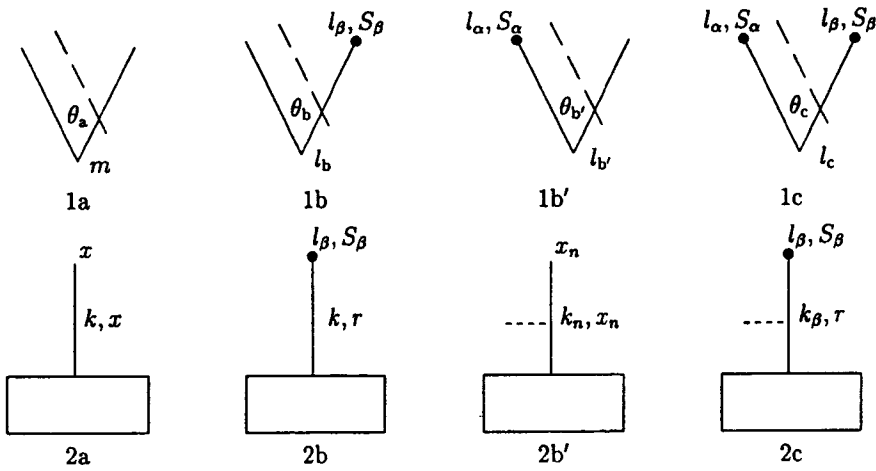


FIG. 4. Elementary cells for  $S_n$  (diagrams 1a,...,1c) and their contractions to  $E_n$  ones (diagrams 2a,...,2c).

To each branching point on the tree diagram, or each circle on the subgroup diagram, we also associate a quantum number  $l_j$  [see Fig. 3(b) for a specific case]. It will determine the eigenvalue  $\lambda$  of the corresponding  $o(k)$  invariant operator according to the formula

$$Y_j \Psi = \Delta_{LB} \Psi = -l_j(l_j + k - 2) \Psi, \tag{2.11}$$

where  $k$  is the dimension of the ambient space above the corresponding vertex on the tree [the same  $k$  as in  $O(k)$ ]. The numbers  $l_j$  are non-negative integers, labeling irreducible representations of  $O(k)$  for  $k \geq 3$ . For  $k=2$ , i.e., the group  $O(2)$ , we have  $l_j = 0, \pm 1, \pm 2, \dots$

### C. The separated eigenfunctions for $S_n$

To specify the separated wave function,

$$\Psi = \prod_{k=1}^n \Psi_k(\theta_k), \tag{2.12}$$

on  $S_n$ , we follow Refs. 9–13 and introduce four types of vertices, or “cells” on a tree, as illustrated in Fig. 4. The first row, diagrams 1a,...,1c, contains elementary  $S_n$  cells. The second row, 2a,...,2c contains  $E_n$  cells, obtained after a contraction, and will be discussed below in Sec. VIA. The dashed lines in row 1 will also be explained below. A circle on diagrams 1a,...,1c denotes a “closed” end, i.e., one that leads to further branches. An open end (no circle) leads directly to a coordinate. For example, in Fig. 3 angles  $\theta_3$ ,  $\theta_4$  and  $\theta_7$  correspond to cells of type “a,”  $\theta_5$  and  $\theta_6$  to cells of type “b,” and  $\theta_1$ ,  $\theta_2$  to cells of type “c.” The angles in the polyspheric coordinate systems satisfy

$$0 \leq \theta_a < 2\pi, \quad 0 \leq \theta_b \leq \pi, \quad -\pi/2 \leq \theta_{b'} \leq \pi/2, \quad 0 \leq \theta_c \leq \pi/2. \tag{2.13}$$

The following numbers are associated with each cell:  $m$ ,  $l$ ,  $l_\beta$ ,  $l_\alpha$  are related to the separation constant corresponding to each vertex,  $S_\alpha$  = number of vertices above vertex  $l_\alpha$ ,  $S_\beta$  = number of vertices above vertex  $l_\beta$ . The numbers  $m$ ,  $l$ ,  $l_\beta$ ,  $l_\alpha$  are all integers, labeling representations of the corresponding rotation subgroup in the chain, i.e., angular momentum type quantum numbers. We have

$$\Delta + c = n' - 2, \tag{2.14}$$

where  $n'$  is the number of end points  $u_i$  connected to the vertex  $\theta_j$  and  $c$  is the number of vertices above and to the left of vertex  $\theta_{b'}$ , or  $\theta_c$ .

Each vertex and each angle  $\theta_i$  provides a "building block"  $\Psi_i(\theta_i)$  for the wave function  $\Psi(\theta_1, \dots, \theta_n)$  of Eq. (2.12). Specifically, we have the following.

(1) Cell of type a:

$$\Psi_m(\theta_a) = \frac{1}{\sqrt{2\pi}} e^{im\theta_a}; \quad m = 0, \pm 1, \pm 2, \dots, \quad 0 \leq \theta_a < 2\pi. \tag{2.15}$$

(2) Cell of type b:

$$\Psi_{n,l_\beta}^\alpha(\theta_b) = N_n^{\alpha,\alpha}(\sin \theta_b)^{l_\beta} P_n^{(\alpha,\alpha)}(\cos \theta_b),$$

$$n = l - l_\beta, \quad \alpha = l_\beta + \frac{S_\beta}{2}, \quad n = 0, 1, 2, \dots, \quad 0 \leq \theta_b \leq \pi, \tag{2.16}$$

where  $P_n^{(\alpha,\beta)}(x)$  is a Jacobi polynomial.

(3) Cell of type b':

$$\Psi_{n,l_\alpha}^\beta(\theta_{b'}) = N_n^{\beta,\beta}(\cos \theta_{b'})^{l_\alpha} P_n^{(\beta,\beta)}(\sin \theta_{b'});$$

$$n = l - l_\alpha, \quad \beta = l_\alpha + \frac{S_\alpha}{2}, \quad n = 0, 1, 2, \dots, \quad -\pi/2 \leq \theta_{b'} \leq \pi/2. \tag{2.17}$$

(4) Cell of type c:

$$\Psi_{n,l_\beta,l_\alpha}^{\alpha,\beta}(\theta_c) = 2^{(\alpha+\beta)/2+1} N_n^{\alpha,\beta}(\sin \theta_c)^{l_\beta} (\cos \theta_c)^{l_\alpha} P_n^{(\alpha,\beta)}(\cos 2\theta_c);$$

$$n = \frac{l - l_\alpha - l_\beta}{2}, \quad \alpha = l_\beta + \frac{S_\beta}{2}, \quad \beta = l_\alpha + \frac{S_\alpha}{2}, \quad n = 0, 1, 2, \dots, \quad 0 \leq \theta_c \leq \pi/2. \tag{2.18}$$

The normalization constants are

$$N_n^{\alpha,\beta} = \sqrt{\frac{(2n + \alpha + \beta + 1)\Gamma(n + \alpha + \beta + 1)n!}{2^{\alpha+\beta+1}\Gamma(n + \alpha + 1)\Gamma(n + \beta + 1)}}. \tag{2.19}$$

We mention that the wave functions (2.16) and (2.17) can also be expressed in terms of Gegenbauer polynomials, using the formula<sup>34</sup>

$$C_n^\lambda(x) = \frac{\Gamma(2\lambda + n)\Gamma(\lambda + 1/2)}{\Gamma(2\lambda)\Gamma(\lambda + n + 1/2)} P_n^{(\lambda - 1/2, \lambda - 1/2)}(x). \tag{2.20}$$

### III. SUBGROUP TYPE COORDINATES ON $E_n$ AND CLUSTER DIAGRAMS

Let us now consider the Euclidean Lie algebra  $e(n)$ , with a basis

$$L_{ik} = x_i \partial_{x_k} - x_k \partial_{x_i}, \quad p_i = \partial_{x_i}, \quad i, k = 1, 2, \dots, n. \tag{3.1}$$

The commutation relations are, as in Eq. (2.6), together with

$$[p_j, L_{ik}] = \delta_{ji} p_k - \delta_{jk} p_i, \quad [p_i, p_k] = 0. \tag{3.2}$$

Subalgebra chains (2.5) will include Euclidean subalgebras  $e(k)$  and rotation subalgebras  $o(k)$ . A possible link in a subalgebra chain is



$$e(n) \supset e(n_1) \oplus e(n_2), \quad n_1 + n_2 = n, \quad n_1 \geq n_2 \geq 1. \tag{3.3}$$

The Casimir operator of  $e(n)$  is

$$\Delta_n = p_1^2 + p_2^2 + \dots + p_n^2. \tag{3.4}$$

Hence, we have  $\Delta_n = \Delta_{n_1} + \Delta_{n_2}$  in the chain and only one of the Euclidean subalgebras (3.3) provides a new invariant operator, say  $e(n_2)$ . Alternatively,  $\Delta_{n_1}$  and  $\Delta_{n_2}$  can replace  $\Delta_n$ . A further possible link in a chain is

$$e(n) \supset o(n), \quad n \geq 2, \tag{3.5}$$

where  $o(n)$  will provide a new [with respect to  $e(n)$ ] invariant operator.

As in the case of the  $O(n)$  group we will introduce diagrams for the  $E(n)$  group to illustrate subgroup chains and subgroup type coordinate systems on  $E_n$  Euclidean spaces. We shall use rectangles ("boxes") to denote  $E(k)$  groups [or  $e(k)$  algebras] and circles to denote  $O(k)$  groups [or  $o(k)$  algebras]. As an example, we give all subgroup chains for  $E(n)$ ,  $1 \leq n \leq 4$  in Fig. 5. Maximality requires that as we go from one level to a higher one, we obey the following rules

(1) From a rectangle representing  $e(n)$ , we can go to two rectangles [see Eq. (3.3)], representing  $e(n_1) \oplus e(n_2)$ , with  $n_1 + n_2 = n$ ,  $n_1 \geq n_2 \geq 1$ , or to a circle [see Eq. (3.5)], representing  $o(n)$  (the same  $n$  as in the rectangle).

(2) From a circle representing  $o(n)$  we can go to two circles, representing  $o(n_1) \oplus o(n_2)$ ,  $n_1 + n_2 = n$ ,  $n_1 \geq n_2 \geq 2$ , or to one circle, representing  $o(n-1)$ ,  $n \geq 3$ .

Now let us consider subgroup type coordinates on the Euclidean space  $E_n$  and introduce diagrams to represent them. We shall call them "cluster diagrams" and they will consist of individual trees of the  $O(k)$  type with a tree "trunk" added, or isolated "trunks," or of clusters of trees with trunks and isolated trunks. The  $E_n$  cluster diagrams are simpler than the  $E(n)$  subgroup diagrams, since  $E(k)$  subgroups that do not contribute new invariant operators will be omitted.

All clusters for  $E_n$ ,  $1 \leq n \leq 4$ , are also shown in Fig. 5. An isolated trunk corresponds to a Cartesian coordinate. A trunk with further branches above it corresponds to a radial coordinate  $r$  satisfying  $0 \leq r < \infty$ . The tree above the trunk is treated exactly as in the case of polyspheric coordinates on  $S_n$  spheres.

As an example let us consider the diagrams in Fig. 3(d); the coordinates in  $E_7$  are

$$\begin{aligned} x_1 &= z, & x_4 &= r_2 \cos \theta_5 \cos \theta_6 \cos \theta_7, \\ x_2 &= r_1 \cos \theta_4, & x_5 &= r_2 \cos \theta_5 \cos \theta_6 \sin \theta_7, \\ x_3 &= r_1 \sin \theta_4, & x_6 &= r_2 \cos \theta_5 \sin \theta_6, & x_7 &= r_2 \sin \theta_5. \end{aligned} \tag{3.6}$$

The prescriptions for writing the complete sets of commuting operators, eigenvalues and eigenfunctions are now quite simple.

To each tree trunk we associate an  $M$ -dimensional Laplace operator, where  $M$  is the number of end points (Cartesian coordinates) above the trunk. We also associate a number  $k \in \mathbb{R} > 0$  with each trunk. The corresponding radial eigenfunction [normalized to the delta function:  $\delta(k' - k)$ ] is

$$\begin{aligned} \Psi_{kl}(r) &= \sqrt{\frac{k}{r^{M-2}}} J_{1+(M-2)/2}(kr), \quad M \geq 2, \\ \Psi_k(z) &= \frac{e^{ikz}}{\sqrt{2\pi}}, \quad M = 1. \end{aligned} \tag{3.7}$$

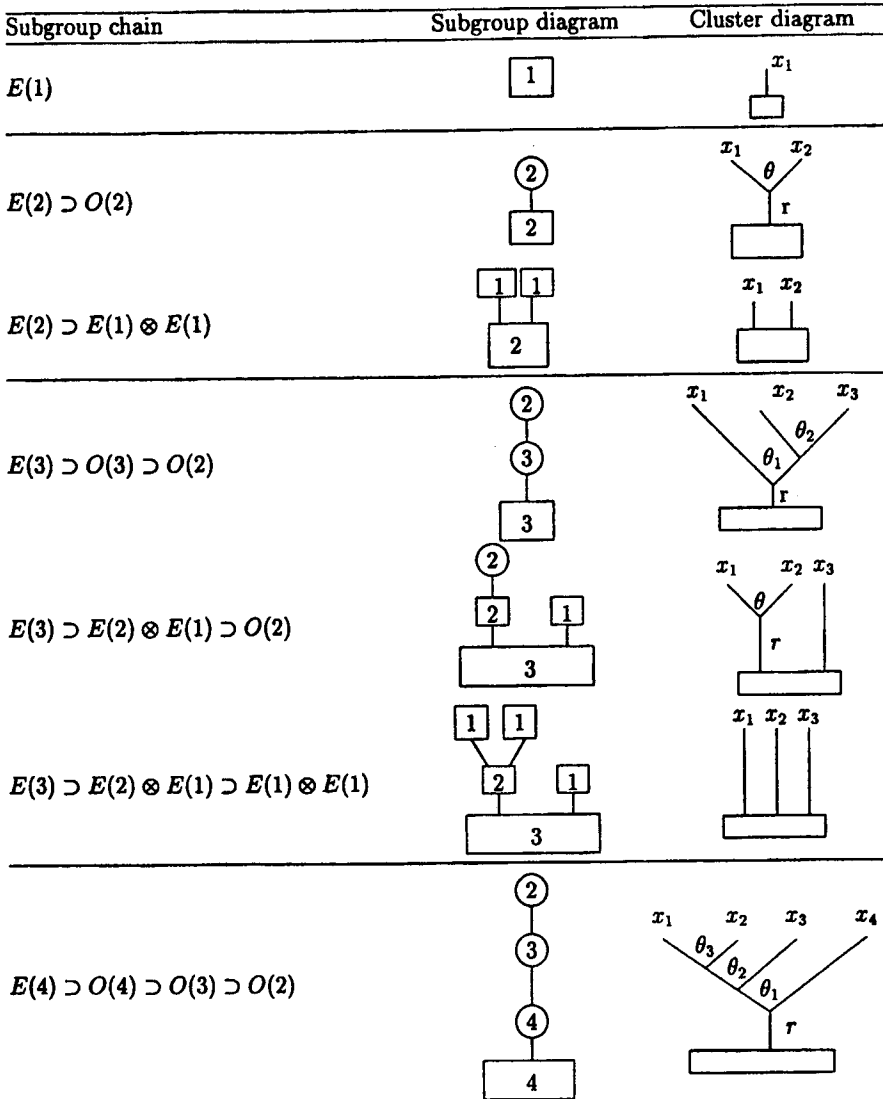


FIG. 5. Subgroup chains for  $E(n)$  and cluster diagrams for  $E_n$ .

The angular part of the eigenfunctions is written following the rules for  $S_n$  spheres, as are the invariant operators and their eigenvalues.

For the example of Figs. 3(c), 3(d), the invariant operators are

$$Y_1 = p_1^2, \quad Y_2 = p_2^2 + p_3^2, \quad Y_3 = p_4^2 + p_5^2 + p_6^2 + p_7^2, \quad Y_4 = L_{23}^2, \tag{3.8}$$

$$Y_5 = L_{45}^2, \quad Y_6 = L_{45}^2 + L_{56}^2 + L_{46}^2, \quad Y_7 = \sum_{4 \leq i < k \leq 7} L_{ik}^2.$$

We note that the Laplace operator on  $E_7$  does not figure explicitly; it is equal to

$$\Delta = \sum_{i=1}^7 p_i^2 = Y_1 + Y_2 + Y_3. \tag{3.9}$$

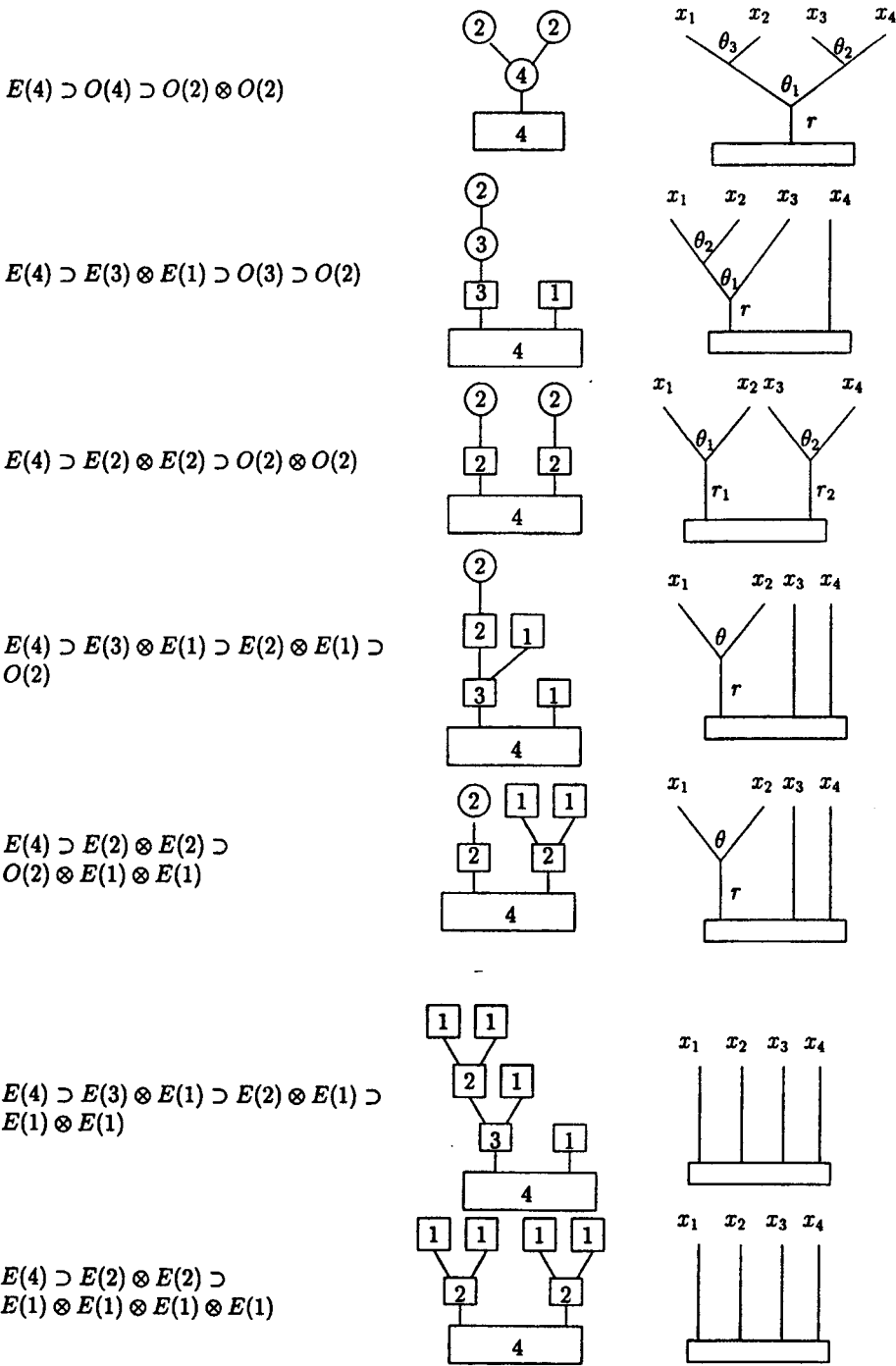


FIG. 5. (Continued.)

#### IV. CONTRACTIONS OF THE LIE ALGEBRA AND CASIMIR OPERATOR

Let us consider the  $n$ -dimensional sphere  $S_n$ :

$$u_0^2 + \sum_{\nu=1}^n u_\nu^2 = \sum_{\mu, \nu=0}^n g_{\mu\nu} u_\mu u_\nu = R^2, \quad R^2 > 0, \quad (4.1)$$

where  $u_\mu$  are Cartesian coordinates in the Euclidean ambient space  $E_{n+1}$  and the metric tensor in this case has the form  $g_{\mu\nu} = \text{diag}(1, 1, \dots, 1)$ . The isometry group is  $O(n+1)$ . We choose a standard basis  $L_{\mu,\nu}$  for the Lie algebra  $o(n+1)$  as in Eq. (2.6).

The Laplace–Beltrami operator on  $S_n$  is

$$\Delta_{LB} = \frac{1}{R^2} \sum_{0 \leq \mu < \nu \leq n} L_{\mu\nu}^2. \tag{4.2}$$

We shall use  $R^{-1}$  as the contraction parameter. To realize the contraction explicitly, let us introduce Beltrami coordinates on the sphere  $S_n$ , putting

$$y_i = R \frac{u_i}{u_0} = u_i \left( 1 - \frac{1}{R^2} \sum_{k=1}^n u_k^2 \right)^{-1/2}, \quad i = 1, 2, 3, \dots, n. \tag{4.3}$$

The  $O(n+1)$  generators then can be expressed as

$$\frac{L_{0i}}{R} \equiv \pi_i = p_i + \frac{y_i}{R^2} \sum_{k=1}^n (y_k p_k), \tag{4.4}$$

$$L_{ik} \equiv y_i p_k - y_k p_i = y_i \pi_k - y_k \pi_i; \quad i, k = 1, 2, \dots, n, \tag{4.5}$$

where  $p_i = \partial/\partial y_i$ . The commutation relations now are

$$[L_{ik}, L_{mn}] = \delta_{km} L_{in} + \delta_{in} L_{km} - \delta_{im} L_{kn} - \delta_{kn} L_{im}, \tag{4.6}$$

$$[\pi_i, L_{kj}] = \delta_{ik} \pi_j - \delta_{ij} \pi_k, \quad [\pi_i, \pi_k] = \frac{L_{ik}}{R^2}, \tag{4.7}$$

so that for  $R \rightarrow \infty$  the  $o(n+1)$  algebra contracts to the Euclidean  $e(n)$  one. The Beltrami coordinates  $y_i$  (4.3) contract to Cartesian coordinates on  $E_n$ , and we have

$$y_i \rightarrow x_i, \quad \pi_i \rightarrow p_i = \frac{\partial}{\partial x_i}, \tag{4.8}$$

so that the rotation generators  $L_{0i}$  go into the translations  $p_i$ .

The  $o(n+1)$  Laplace–Beltrami operator (2.1) contracts to the  $e(n)$  one:

$$\Delta_{LB} = \sum_{i=1}^n \pi_i^2 + \sum_{i,k=1}^n \frac{L_{ik}^2}{2R^2} \rightarrow \Delta = p_1^2 + p_2^2 + \dots + p_n^2. \tag{4.9}$$

## V. CONTRACTION AND COORDINATE SYSTEMS. THE GRAPHICAL METHOD

### A. General formulation

We have seen that all subgroup type coordinates on a sphere  $S_n$  can be characterized by tree diagrams. Similarly, there is a one-to-one correspondence between subgroup type coordinates in a Euclidean space  $E_n$  and the cluster diagrams of Sec. IV.

We shall now introduce a *graphical method* for connecting the subgroup type coordinate systems on  $S_n$  and  $E_n$  and give the rules relating the coordinates, invariant operators, eigenvalues and basis functions. The relations are asymptotic ones for the radius of the sphere satisfying  $R \rightarrow \infty$  and one, or more, of the angles  $\theta_i$  satisfying  $\theta_i \rightarrow 0$ .

A general  $S_n$  tree diagram can be represented by Fig. 6(a). One principal branch of the tree goes from the ground to the point representing the coordinate  $u_0$ . The branches growing from this one can lead directly to a coordinate  $u_i$ , or they can branch further and lead to sets of coordinates,

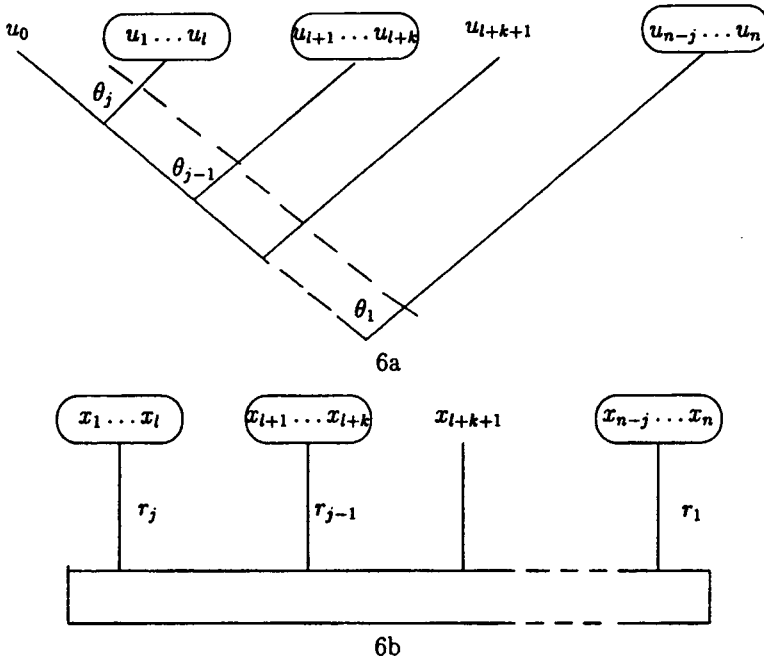


FIG. 6. Contractions of tree diagrams into cluster ones for  $S_n \rightarrow E_n$ .

e.g.,  $\{u_{l+1}, u_{l+2}, \dots, u_{l+k}\}$ . Graphically the contraction  $R \rightarrow \infty$  corresponds to the fact that we cut off the ground to  $u_0$  branch by the dashed line in Fig. 6(a). The dashed line then becomes the ground for the corresponding cluster  $E_n$  diagram of Fig. 6(b) and the ambient space coordinates  $(u_0, u_1, \dots, u_n)$  for  $S_n$  are replaced by the Cartesian coordinates  $(x_1, x_2, \dots, x_n)$ . The angles  $\theta_1, \theta_2, \dots, \theta_j$  that lead to branches cut-off by the dotted line satisfy  $\theta_i \rightarrow 0$  in the contraction and are replaced by radial coordinates  $r_i$ , or Cartesian coordinates  $x_m$  (if the surviving branch leads directly to a single coordinate on  $S_n$  and  $E_n$ ). We have

$$R \rightarrow \infty, \quad \theta_i \rightarrow 0, \quad R \tan \theta_i \sim R \sin \theta_i \sim R \theta_i \rightarrow r_i. \tag{5.1}$$

The individual trees in an  $E_n$  cluster correspond to  $O(k)$  subgroups of  $O(n)$  that survive the contraction.

All contractions of coordinate systems for  $S_1, S_2,$  and  $S_3$  are illustrated in Fig. 7. Let us run through the individual cases.

**B. Contractions from  $S_1$  to  $E_1$**

In the case of a one-dimensional sphere, i.e., a circle, we have only one diagram, namely No. 1 of Fig. 7. In the original ambient space we have polar coordinates

$$u_0 = R \cos \theta, \quad u_1 = R \sin \theta, \tag{5.2}$$

with  $0 \leq \theta < 2\pi$ . The Beltrami coordinate satisfies

$$y_1 = R \tan \theta \rightarrow x, \tag{5.3}$$

where  $x$  is a Cartesian coordinate on  $E_1$ .

**C. Contractions from  $S_2$  to  $E_2$**

In the case of the two-dimensional sphere  $S_2$  we have two tree configurations and two types of coordinate contractions to consider, namely, No. 2 and No. 3 of Fig. 7.

| No | Cut tree diagram | Cluster diagram | Contraction of coordinates |
|----|------------------|-----------------|----------------------------|
| 1  |                  |                 | Polar to Cartesian         |
| 2  |                  |                 | Spherical to Spherical     |
| 3  |                  |                 | Spherical to Cartesian     |
| 4  |                  |                 | Spherical to Spherical     |
| 4' |                  |                 | Spherical to Spherical     |
| 5  |                  |                 | Spherical to Cylindrical   |
| 6  |                  |                 | Spherical to Cartesian     |
| 7  |                  |                 | Cylindrical to Cylindrical |

FIG. 7. Contractions of tree diagrams on  $S_n$  into cluster ones on  $E_n$  for  $1 \leq n \leq 4$ .

For diagram No. 2 we have

$$u_0 = R \cos \theta_1, \quad u_1 = R \sin \theta_1 \cos \theta_2, \quad u_2 = R \sin \theta_1 \sin \theta_2, \quad (5.4)$$

where  $0 \leq \theta_1 < \pi$ ,  $0 \leq \theta_2 < 2\pi$ . Introducing Beltrami coordinates and taking the appropriate limits  $R \rightarrow \infty$ ,  $\theta_1 \sim r/R$ , we have

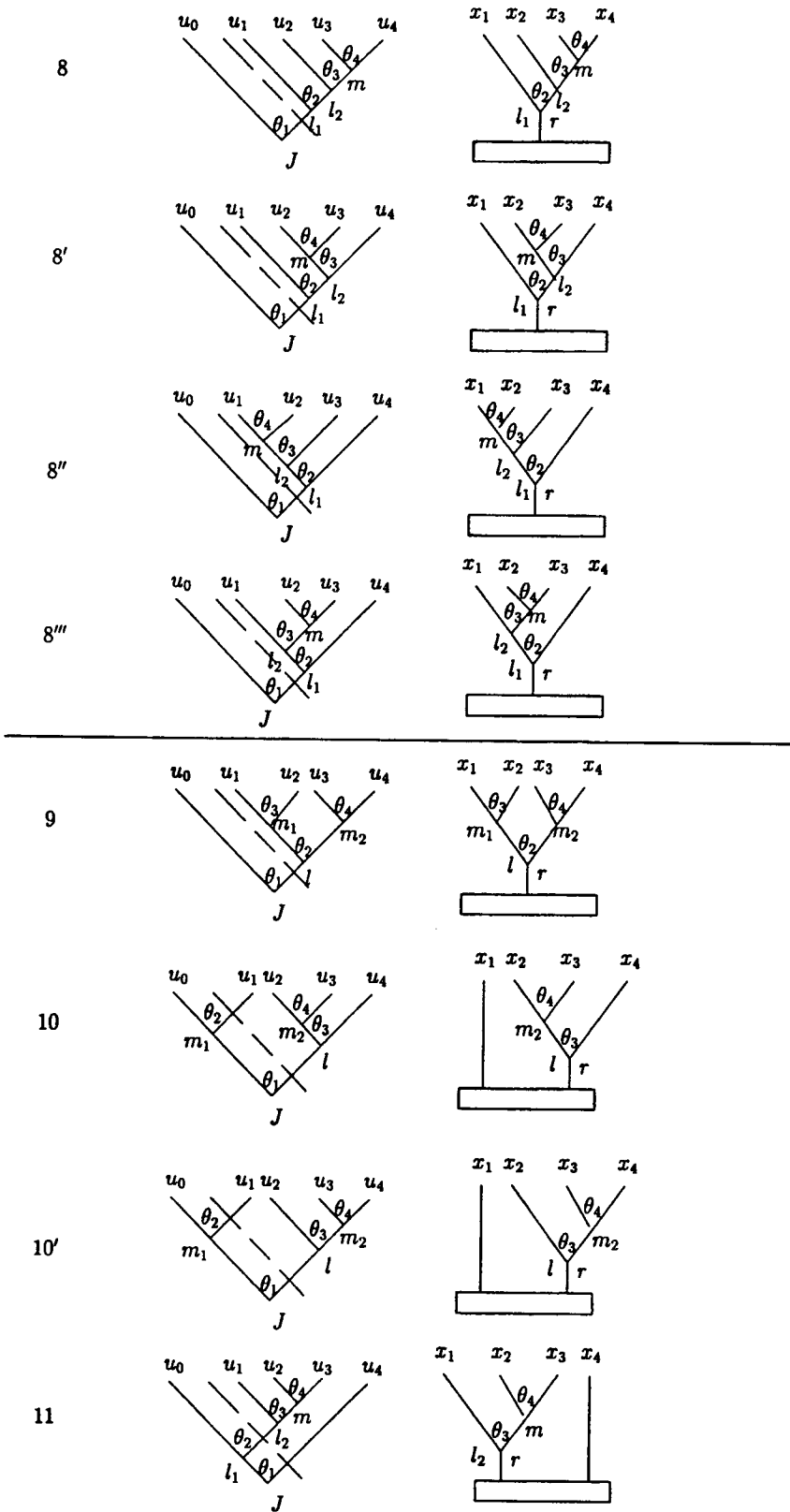


FIG. 7. (Continued.)

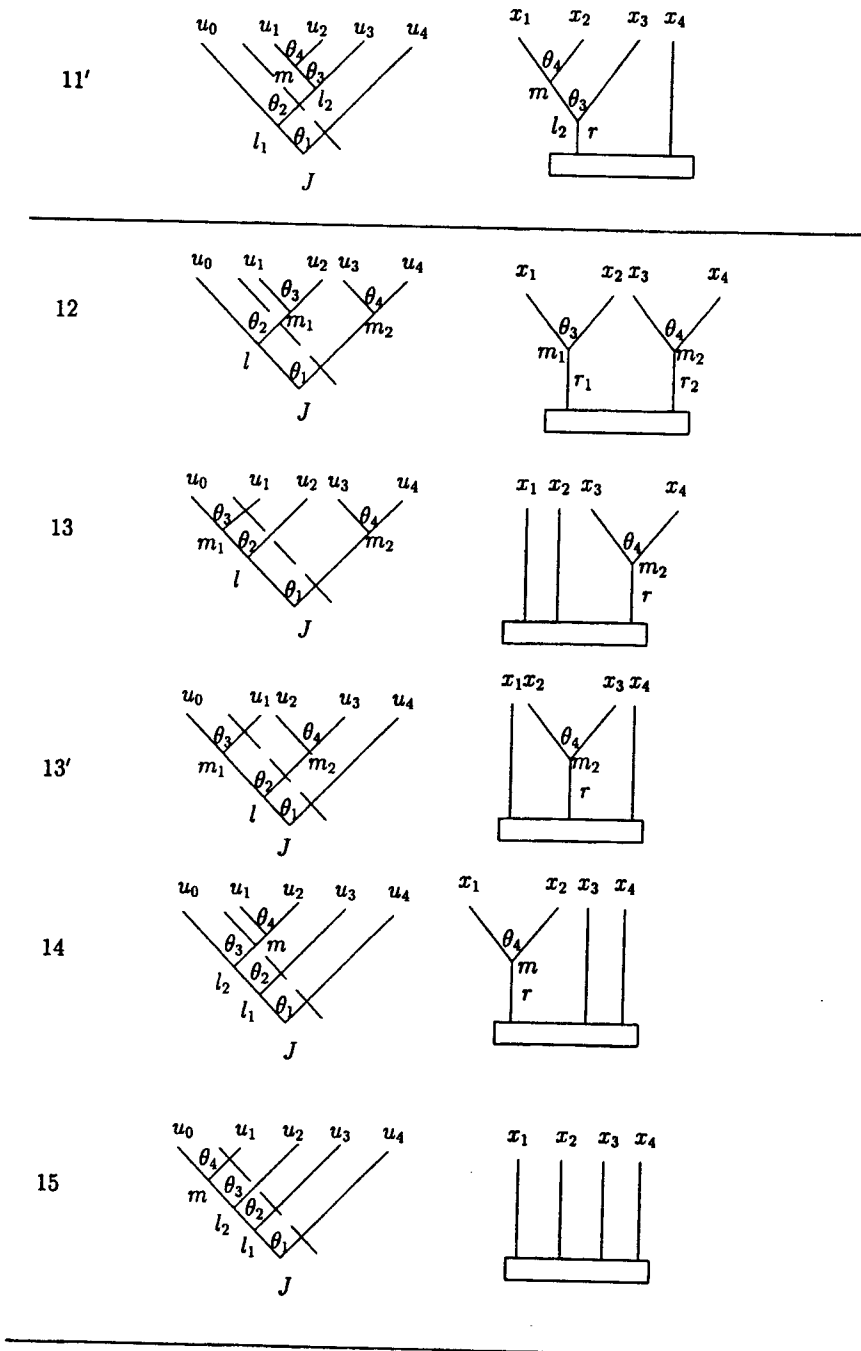


FIG. 7. (Continued.)

$$y_1 = R \tan \theta_1 \cos \theta_2 \rightarrow x_1 = r \cos \theta_2, \quad y_2 = R \tan \theta_1 \sin \theta_2 \rightarrow x_2 = r \sin \theta_2. \quad (5.5)$$

The subgroup chain  $O(3) \supset O(2)$  contracts to the Euclidean one:  $E(2) \supset O(2)$ ; the  $O(2)$  invariant and its eigenvalues  $m$  survive the contraction  $L_{12}^2 \rightarrow L_{12}^2$ ,  $m \rightarrow m$ .

For diagram No. 3 in Fig. 7 we have

$$u_0 = R \cos \theta_1 \cos \theta_2, \quad u_1 = R \cos \theta_1 \sin \theta_2, \quad u_2 = R \sin \theta_1, \quad (5.6)$$



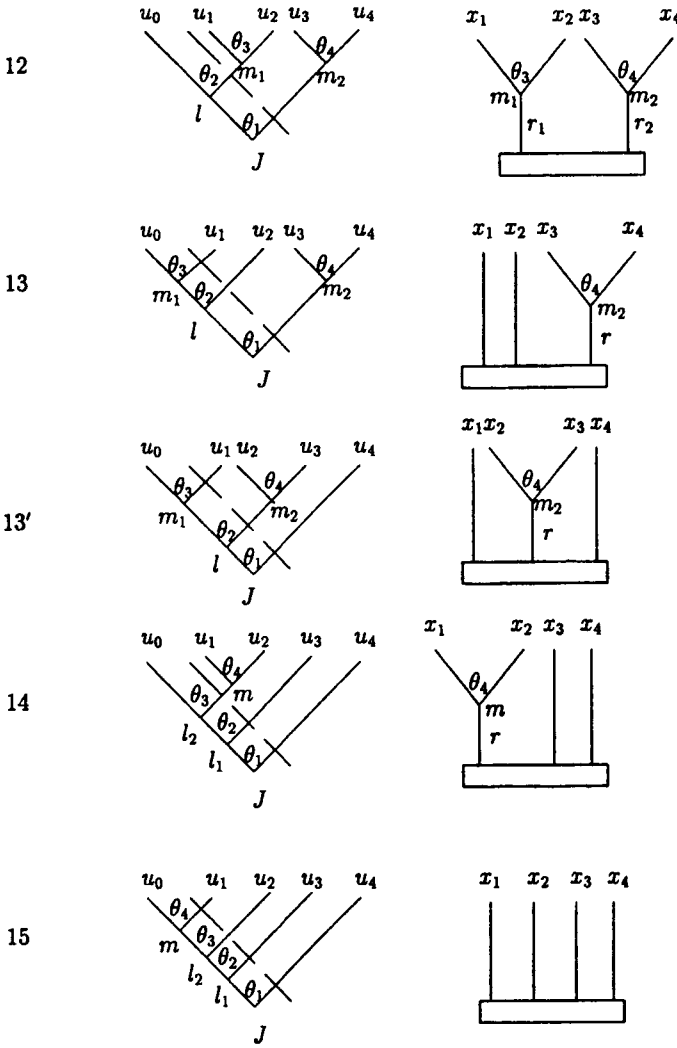


FIG. 7. (Continued.)

and the Beltrami coordinates satisfy ( $R \rightarrow \infty$ ,  $\theta_1 \sim x_1/R$ ,  $\theta_2 \sim x_2/R$ )

$$y_1 = R \tan \theta_2 \rightarrow x_1, \quad y_2 = R \frac{\tan \theta_1}{\cos \theta_2} \rightarrow x_2. \tag{5.7}$$

The subgroup chain  $O(3) \supset O(2)$  contracts to  $E(2) \supset E(1) \otimes E(1)$  and the  $O(2)$  subgroup invariant undergoes a contraction,

$$\frac{Y_1}{R^2} = \frac{L_{01}^2}{R^2} = \pi_1^2 \rightarrow p_1^2. \tag{5.8}$$

**D. Contractions from  $S_3$  to  $E_3$**

Five types of  $O(4)$  tree diagrams exist, but only four of them give different contractions.

The diagrams No. 4 and 4' on Fig. 7 correspond to spherical coordinates on  $S_3$  going into spherical coordinates on  $E_3$ . For No. 4 the polyspherical coordinates are

$$\begin{aligned}
 u_0 &= R \cos \theta_1, & u_1 &= R \sin \theta_1 \cos \theta_2, \\
 u_2 &= R \sin \theta_1 \sin \theta_2 \cos \theta_3, & u_3 &= R \sin \theta_1 \sin \theta_2 \sin \theta_3.
 \end{aligned}
 \tag{5.9}$$

The Beltrami coordinates satisfy  $(R \rightarrow \infty, \theta_1 \sim r/R)$

$$\begin{aligned}
 y_1 &= R \tan \theta_1 \cos \theta_2 \rightarrow x_1 = r \cos \theta_2, \\
 y_2 &= R \tan \theta_1 \sin \theta_2 \cos \theta_3 \rightarrow x_2 = r \sin \theta_2 \cos \theta_3, \\
 y_3 &= R \tan \theta_1 \sin \theta_2 \sin \theta_3 \rightarrow x_3 = r \sin \theta_2 \sin \theta_3.
 \end{aligned}
 \tag{5.10}$$

We have  $O(4) \supset O(3) \supset O(2) \rightarrow E(3) \supset O(3) \supset O(2)$  so that the  $O(3) \supset O(2)$  subgroups and their invariants survive:

$$Y_1 = L^2 = L_{12}^2 + L_{13}^2 + L_{23}^2 \rightarrow L^2, \quad Y_2 = L_{23}^2 \rightarrow L_{23}^2.
 \tag{5.11}$$

The situation for diagram No. 4' is quite analogous.

The case No. 5 in Fig. 7 corresponds to spherical coordinates contracting to cylindrical ones. We have

$$\begin{aligned}
 u_0 &= R \cos \theta_1 \cos \theta_2, & u_1 &= R \cos \theta_1 \sin \theta_2 \cos \theta_3, \\
 u_2 &= R \cos \theta_1 \sin \theta_2 \sin \theta_3, & u_3 &= R \sin \theta_1.
 \end{aligned}
 \tag{5.12}$$

For Beltrami coordinates  $(R \rightarrow \infty, \theta_2 \sim r/R, \theta_1 \sim x_3/R)$  we obtain

$$\begin{aligned}
 y_1 &= R \tan \theta_2 \cos \theta_3 \rightarrow x_1 = r \cos \theta_3, \\
 y_2 &= R \tan \theta_2 \sin \theta_3 \rightarrow x_2 = r \sin \theta_3, \\
 y_3 &= R \frac{\tan \theta_1}{\cos \theta_2} \rightarrow x_3 = z.
 \end{aligned}
 \tag{5.13}$$

The subgroup chain contraction is  $O(4) \supset O(3) \supset O(2) \rightarrow E(3) \supset E(2) \otimes E(1) \supset O(2)$  and the subgroup invariants contract as

$$\frac{Y_1}{R^2} = \frac{1}{R^2} (L_{01}^2 + L_{02}^2 + L_{12}^2) = \pi_1^2 + \pi_2^2 + \frac{L_{12}^2}{R^2} \rightarrow p_1^2 + p_2^2, \quad Y_2 = L_{12}^2 \rightarrow L_{12}^2.
 \tag{5.14}$$

The diagram No. 6 in Fig. 7 corresponds to the contraction of spherical coordinates to Cartesian ones. We have

$$\begin{aligned}
 u_0 &= R \cos \theta_1 \cos \theta_2 \cos \theta_3, & u_1 &= R \cos \theta_1 \cos \theta_2 \sin \theta_3, \\
 u_2 &= R \cos \theta_1 \sin \theta_2, & u_3 &= R \sin \theta_1.
 \end{aligned}
 \tag{5.15}$$

For Beltrami coordinates after the contraction  $R \rightarrow \infty, \theta_3 \sim x_1/R, \theta_2 \sim x_2/R, \theta_1 \sim x_3/R$ , we have

$$y_1 = R \tan \theta_3 \rightarrow x_1, \quad y_2 = R \frac{\tan \theta_2}{\cos \theta_3} \rightarrow x_2, \quad y_3 = R \frac{\tan \theta_1}{\cos \theta_2 \cos \theta_3} \rightarrow x_3.
 \tag{5.16}$$

The subgroup chain undergoes the contraction  $O(4) \supset O(3) \supset O(2) \rightarrow E(3) \supset E(1) \otimes E(1) \otimes E(1)$  and the subgroup invariants satisfy

$$\frac{Y_1}{R^2} = \frac{1}{R^2}(L_{01}^2 + L_{02}^2 + L_{12}^2) = \pi_1^2 + \pi_2^2 = \frac{L_{12}^2}{R^2} \rightarrow p_1^2 + p_2^2, \quad \frac{Y_2}{R^2} = \frac{L_{01}^2}{R^2} = \pi_1^2 \rightarrow p_1^2. \quad (5.17)$$

Finally the diagram No. 7 of Fig. 7 corresponds to polyspherical (or cylindrical) coordinates on  $S_3$  contracting to cylindrical ones on  $E_3$ . We have

$$\begin{aligned} u_0 &= R \cos \theta_1 \cos \theta_2, & u_1 &= R \cos \theta_1 \sin \theta_2, \\ u_2 &= R \sin \theta_1 \cos \theta_3, & u_3 &= R \sin \theta_1 \sin \theta_3. \end{aligned} \quad (5.18)$$

For the Beltrami coordinates after the contraction  $R \rightarrow \infty$ ,  $\theta_2 \sim x_1/R$ ,  $\theta_1 \sim r/R$ , we obtain

$$\begin{aligned} y_1 &= R \tan \theta_2 \rightarrow x_1, \\ y_2 &= R \tan \theta_1 \frac{\cos \theta_3}{\cos \theta_2} \rightarrow x_2 = r \cos \theta_3, \\ y_3 &= R \tan \theta_1 \frac{\sin \theta_3}{\cos \theta_2} \rightarrow x_3 = r \sin \theta_3. \end{aligned} \quad (5.19)$$

The subgroup chain satisfies  $O(4) \supset O(2) \oplus O(2) \rightarrow E(3) \supset E(2) \oplus E(1) \supset O(2)$  so that for the subgroup invariants we have

$$\frac{Y_1}{R^2} = \frac{L_{01}^2}{R^2} = \pi_1^2 \rightarrow p_1^2, \quad Y_2 = L_{23}^2 \rightarrow L_{23}^2. \quad (5.20)$$

## VI. CONTRACTIONS OF BASIS FUNCTIONS

### A. Contractions of functions corresponding to elementary cells

When we cut off the branches of a tree as in Fig. 6, the cutting line intersects an elementary cell (see Fig. 4) at each branch. Each elementary  $O(n+1)$  cell then goes into an elementary trunk for  $E(n)$ , as indicated by the lower row of diagrams in Fig. 4.

Let us now discuss the four cases in Fig. 4. The limiting procedure is always the same, namely,

$$\theta_j \sim \frac{r_j}{R}, \quad l_j \sim kR, \quad R \rightarrow \infty, \quad j = a, b, b', c, \quad (6.1)$$

where  $r_j$  is the radius of the sphere that survives the contraction, i.e., corresponds to the circle on the right hand side of the  $O(n+1)$  cell and on top of the  $E(n)$  trunk. Thus, for  $j = a$  and  $j = b'$  we have  $r_j = x$ , a Cartesian coordinate. Similarly, we have  $l_\alpha = m \in \mathbb{Z}$  and also  $l_\beta = m \in \mathbb{Z}$ .

Let us now run through the individual cells in Fig. 4.

#### 1. Cell 1a to 2a

Using Eqs. (2.15) and (6.1) we have ( $R \rightarrow \infty, m \sim kR, \theta \sim x/R$ )

$$\lim_{R \rightarrow \infty} \frac{1}{\sqrt{2\pi}} e^{im\theta_a} = \frac{1}{\sqrt{2\pi}} e^{ikx}. \quad (6.2)$$

#### 2. Cell 1b to 2b

The contribution to the separated  $O(n+1)$  basis function is given in Eq. (2.16). Using the formula for Jacobi polynomials in terms of the hypergeometric functions,<sup>34</sup> we have

$$\begin{aligned}
 & N_{l-l_\beta}^{l_\beta+S_\beta/2, l_\beta+S_\beta/2}(\sin \theta_b) {}_l P_{l-l_\beta}^{(l_\beta+S_\beta/2, l_\beta+S_\beta/2)}(\cos \theta_b) \\
 &= \sqrt{\frac{(2l+S_\beta+1)(l+l_\beta+S_\beta)!}{2(l-l_\beta)!}} \\
 & \cdot \frac{(\sin \theta_b)^{l_\beta}}{2^{l_\beta+S_\beta/2} \Gamma(l_\beta+S_\beta/2+1)} {}_2F_1\left(-l+l_\beta, l+l_\beta+S_\beta+1; l_\beta+\frac{S_\beta}{2}+1; \sin^2 \frac{\theta_b}{2}\right). \quad (6.3)
 \end{aligned}$$

Now, using the asymptotic formulas for the hypergeometric and  $\Gamma$  functions ( $l \sim kR, \theta_b \sim r/R$ ),

$$\lim_{R \rightarrow \infty} {}_2F_1\left(-l+l_\beta, l+l_\beta+S_\beta+1; l_\beta+\frac{S_\beta}{2}+1; \sin^2 \frac{\theta_b}{2}\right) = {}_0F_1\left(l_\beta+\frac{S_\beta}{2}+1; -\frac{k^2 r^2}{4}\right), \quad (6.4)$$

$$\lim_{|z| \rightarrow \infty} \frac{\Gamma(z+\alpha)}{\Gamma(z+\beta)} = z^{\alpha-\beta} \left(1 + \frac{1}{2z}(\alpha-\beta)(\alpha+\beta-1) + O(z^{-2})\right), \quad (6.5)$$

and the formula for the Bessel function,

$$J_\nu(z) = \left(\frac{z}{2}\right)^\nu \frac{1}{\Gamma(\nu+1)} {}_0F_1\left(\nu+1; -\frac{z^2}{4}\right), \quad (6.6)$$

we obtain

$$\lim_{R \rightarrow \infty} \frac{1}{\sqrt{R^{S_\beta+1}}} N_{l-l_\beta}^{l_\beta+S_\beta/2, l_\beta+S_\beta/2}(\sin \theta_b) {}_l P_{l-l_\beta}^{(l_\beta+S_\beta/2, l_\beta+S_\beta/2)}(\cos \theta_b) = \sqrt{\frac{k}{r^{S_\beta}}} J_{l_\beta+S_\beta/2}(kr). \quad (6.7)$$

### 3. Cell 1b' to 2b'

The contribution of this cell to the  $O(n+1)$  separated basis function is given in Eq. (2.17). In order to take the contraction limit (6.1) we express the Jacobi polynomials in terms of hypergeometric functions:<sup>34</sup>

$$\begin{aligned}
 P_n^{(\alpha, \alpha)}(x) &= \frac{2^{2\alpha}}{\sqrt{\pi}} \frac{\Gamma(n+\alpha+1)}{\Gamma(n+2\alpha+1)} \\
 & \times \begin{cases} (-1)^{n/2} \frac{\Gamma([n+1]/2+\alpha)}{\Gamma(n/2+1)} {}_2F_1\left(-\frac{n}{2}, \frac{n+1}{2}+\alpha; \frac{1}{2}; x^2\right), & n \text{ even,} \\ (-1)^{(n-1)/2} \frac{\Gamma(n/2+\alpha+1)}{\Gamma([n+1]/2)} {}_2x_2F_1\left(-\frac{n-1}{2}, \frac{n+2}{2}+\alpha; \frac{3}{2}; x^2\right), & n \text{ odd.} \end{cases} \quad (6.8)
 \end{aligned}$$

In the limit  $R \rightarrow \infty$  and  $\theta_b \sim x_n/R, l \sim kR, l_\alpha \sim pR$ , we have

$$\begin{aligned}
 & \lim_{R \rightarrow \infty} (-1)^{(l-l_\alpha)/2} N_{l-l_\alpha}^{l_\alpha+S_\alpha/2, l_\alpha+S_\alpha/2}(\cos \theta_b) {}_l P_{l-l_\alpha}^{(l_\alpha+S_\alpha/2, l_\alpha+S_\alpha/2)}(\sin \theta_b) \\
 &= \sqrt{\frac{2k}{\pi k_n}} \times \begin{cases} {}_0F_1\left(\frac{1}{2}; \frac{-k_n^2 x_n^2}{4}\right), \\ -i(k_n x_n) {}_0F_1\left(\frac{3}{2}; \frac{-k_n^2 x_n^2}{4}\right), \end{cases} \quad (6.9)
 \end{aligned}$$

where  $k^2 = p^2 + k_n^2$ . The  ${}_0F_1(x)$  hypergeometric functions in this case are expressible in terms of  $\sin k_n x_n$  and  $\cos k_n x_n$  functions,<sup>34</sup>

$${}_0F_1\left(\frac{1}{2}; -\frac{k_n^2 x_n^2}{4}\right) = \cos k_n x_n, \quad {}_0F_1\left(\frac{3}{2}; -\frac{k_n^2 x_n^2}{4}\right) = \sin k_n x_n, \tag{6.10}$$

and we finally have

$$\lim_{R \rightarrow \infty} (-1)^{(l-l_\alpha)/2} N_{l-l_\alpha}^{l_\alpha+S_\alpha/2, l_\alpha+S_\alpha/2}(\cos \theta_{b'})^{l_\alpha} P_{l-l_\alpha}^{(l_\alpha+S_\alpha/2, l_\alpha+S_\alpha/2)}(\sin \theta_{b'}) = \sqrt{\frac{2k}{\pi k_n}} \begin{Bmatrix} \cos(k_n x_n) \\ -i \sin(k_n x_n) \end{Bmatrix}. \tag{6.11}$$

**4. Cell 1c to 2c**

The relevant basis function is given in Eq. (2.18). To take the limit (6.1),  $l \sim kR$ ,  $l_\alpha \sim k_\alpha R$  and  $\theta \sim r/R$ , we use the equation expressing Jacobi polynomials in terms of hypergeometric functions, and take the limit leading to Bessel functions:

$$\begin{aligned} &\lim_{R \rightarrow \infty} \frac{\Gamma([l-l_\alpha-l_\beta]/2+1)}{\Gamma([l-l_\alpha+l_\beta+S_\beta]/2+1)} P_{(l-l_\alpha-l_\beta)/2}^{(l_\beta+S_\beta/2, l_\alpha+S_\alpha/2)}(\cos 2\theta_c) \\ &= \lim_{R \rightarrow \infty} \frac{1}{\Gamma(l_\beta+S_\beta/2+1)} {}_2F_1\left(-\frac{l-l_\alpha-l_\beta}{2}, \frac{l+l_\alpha+l_\beta+S_\alpha+S_\beta}{2}+1; l_\beta+\frac{S_\beta}{2}+1; \sin^2 \theta_c\right) \\ &= \frac{1}{\Gamma(l_\beta+S_\beta/2+1)} {}_0F_1\left(l_\beta+\frac{S_\beta}{2}+1; -\frac{k_\beta^2 r^2}{4}\right) = \left(\frac{2}{k_\beta r}\right)^{l_\beta+S_\beta/2} J_{l_\beta+S_\beta/2}(k_\beta r), \end{aligned} \tag{6.12}$$

where  $k_\alpha^2 + k_\beta^2 = k^2$ . The final result is

$$\begin{aligned} &\lim_{R \rightarrow \infty} \frac{2^{(l_\alpha+S_\alpha/2+l_\beta+S_\beta/2)/2+1}}{\sqrt{R^{S_\beta+1}}} N_{(l-l_\alpha-l_\beta)/2}^{l_\beta+S_\beta/2, l_\alpha+S_\alpha/2}(\sin \theta_c)^{l_\beta} (\cos \theta_c)^{l_\alpha} P_{(l-l_\alpha-l_\beta)/2}^{(l_\beta+S_\beta/2, l_\alpha+S_\alpha/2)}(\cos 2\theta_c) \\ &= \sqrt{\frac{2k}{r S_\beta}} J_{l_\beta+S_\beta/2}(k_\beta r). \end{aligned} \tag{6.13}$$

These contractions for basis functions of the elementary cells (1a,...,1c) determine the general contractions for hyperspherical functions corresponding to any tree for the sphere  $S_n$ .

**B. Examples**

The contraction formulas for basis functions of  $O(3)$  were given in Ref. 1. Here we apply the general rules to give all different  $S_3$  and  $S_4$  contraction diagrams in Fig. 7.

**1. The  $S_3$  sphere**

(1) Polyspherical to spherical coordinates [see Figs. 7(4)–7(4')] ( $R \rightarrow \infty$ ,  $J \sim kR$ ),

$$\lim_{R \rightarrow \infty} \frac{1}{R} \Psi_{Jlm}(\theta_1, \theta_2, \theta_3) = \sqrt{\frac{k}{r}} J_{l+1/2}(kr) Y_{lm}(\theta_2, \theta_3), \tag{6.14}$$

where  $Y_{lm}(\theta_2, \theta_3)$  is a spherical function on  $S_2$ .

(2) Polyspherical to cylindrical coordinates [see Fig. 7(5)] ( $R \rightarrow \infty$ ,  $J \sim kR$ ,  $l \sim k_3/R$ ),

$$\lim_{R \rightarrow \infty} \frac{(-1)^{(J-l)/2}}{\sqrt{R}} \Psi_{Jlm}(\theta_1, \theta_2, \theta_3) = \sqrt{\frac{kp}{\pi k_3}} J_{|m|}(pr) \frac{e^{im\theta_3}}{\sqrt{2\pi}} \begin{Bmatrix} \cos k_3 z \\ -i \sin k_3 z \end{Bmatrix}, \tag{6.15}$$

where  $k^2 = k_3^2 + p^2$ .

(3) Polyspherical to Cartesian coordinates [see Fig. 7(6)] ( $R \rightarrow \infty, J \sim k_1 R, l \sim k_2 / R, m \sim k_3 R$ )

$$\lim_{R \rightarrow \infty} (-1)^{(J-m)/2} \Psi_{Jlm}(\theta_1, \theta_2, \theta_3) = \sqrt{\frac{2}{\pi k_1 k_3}} \frac{e^{ik_1 x}}{\pi} \left\{ \begin{array}{l} \cos k_2 y \cos k_3 z \\ -i \sin k_2 y \cos k_3 z \\ -i \cos k_2 y \sin k_3 z \\ -\sin k_2 y \sin k_3 z \end{array} \right\}, \quad (6.16)$$

where  $k^2 = k_1^2 + k_2^2 + k_3^2$ .

(4) Polyspherical (cylindrical) to cylindrical coordinates [see Fig. 7(7)] ( $R \rightarrow \infty, J \sim kR, m \sim k_3 R$ )

$$\lim_{R \rightarrow \infty} \frac{1}{\sqrt{R}} \Psi_{Jm_1 m_2}(\theta_1, \theta_2, \theta_3) = \sqrt{\frac{k}{\pi}} J_{|m_2|}(pr) e^{ik_3 z} \frac{e^{im_2 \theta_3}}{\sqrt{2\pi}}, \quad (6.17)$$

where  $k^2 = k_3^2 + p^2$ .

## 2. The $S_4$ sphere

(1) Polyspherical to polyspherical coordinates [see Figs. 7(8)–7(8<sup>m</sup>)] ( $R \rightarrow \infty, J \sim kR$ ),

$$\lim_{R \rightarrow \infty} \frac{1}{\sqrt{R^3}} \Psi_{Jl_1 l_2 m}(\theta_1, \theta_2, \theta_3, \theta_4) = \frac{\sqrt{k}}{r} J_{l_1+1}(kr) \Psi_{l_1 l_2 m}(\theta_2, \theta_3, \theta_4), \quad (6.18)$$

where  $\Psi_{l_1 l_2 m}(\theta_2, \theta_3, \theta_4)$  is a hyperspherical function on  $S_3$ .

(2) Polyspherical to cylindrical coordinates [see Fig. 7(9)] ( $R \rightarrow \infty, J \sim kR$ ),

$$\lim_{R \rightarrow \infty} \frac{1}{\sqrt{R^3}} \Psi_{Jl_1 m_1 m_2}(\theta_1, \theta_2, \theta_3, \theta_4) = \frac{\sqrt{k}}{r} J_{l_1+1}(kr) \Psi_{l_1 m_1 m_2}(\theta_2, \theta_3, \theta_4), \quad (6.19)$$

where  $\Psi_{l_1 m_1 m_2}(\theta_2, \theta_3, \theta_4)$  is a hyperspherical function on  $S_3$ .

(3) Polyspherical to four-dimensional cylindrical coordinates in Fig. 7(10) [see also Fig. 7(10') ] ( $R \rightarrow \infty, J \sim kR, m_1 \sim k_1 R$ ),

$$\lim_{R \rightarrow \infty} \frac{1}{R} \Psi_{Jl_1 m_1 m_2}(\theta_1, \theta_2, \theta_3, \theta_4) = \sqrt{\frac{k}{\pi r}} e^{ik_1 x_1} J_{l_1+1/2}(pr) Y_{l_1 m_2}(\pi/2 - \theta_3, \theta_4), \quad (6.20)$$

where  $Y_{l_1 m_2}(\pi/2 - \theta_3, \theta_4)$  is a spherical function on  $S_2$  and  $k^2 = k_1^2 + p^2$ .

(4) Polyspherical to four-dimensional cylindrical coordinates in Fig. 7(11) [see also Fig. 7(11') ] ( $R \rightarrow \infty, J \sim kR, l \sim k_4 R$ ),

$$\lim_{R \rightarrow \infty} \frac{(-1)^{(J-l)/2}}{R} \Psi_{Jl_1 l_2 m}(\theta_1, \theta_2, \theta_3, \theta_4) = \sqrt{\frac{2pk}{\pi k_4 r}} J_{l_2+1/2}(pr) Y_{l_2 m}(\theta_3, \theta_4) \left\{ \begin{array}{l} \cos(k_4 x_4) \\ -i \sin(k_4 x_4) \end{array} \right\}, \quad (6.21)$$

where  $Y_{l_2 m}(\theta_3, \theta_4)$  is a spherical function on  $S_2$  and  $k^2 = k_4^2 + p^2$ .

(5) Polyspherical to bipolar coordinates in Fig. 7(12) ( $R \rightarrow \infty, J \sim kR, l \sim k_1 R$ ),

$$\lim_{R \rightarrow \infty} \frac{1}{R} \Psi_{Jl_1 m_1 m_2}(\theta_1, \theta_2, \theta_3, \theta_4) = \frac{\sqrt{2kk_1}}{2\pi} J_{m_1}(k_1 r_1) J_{m_2}(k_2 r_2) e^{im_1 \theta_3 + im_2 \theta_4}, \quad (6.22)$$

where  $k_1^2 + k_2^2 = k^2$ .

(6) Polyspherical to double cylindrical coordinates in Fig. 7(13) [see also Fig. 7(13')] ( $R \rightarrow \infty, J \sim kR, l \sim k_1R, m \sim k_2R$ ),

$$\lim_{R \rightarrow \infty} \frac{(-1)^{(l-m)/2}}{\sqrt{R}} \Psi_{Jl_1 m_2}(\theta_1, \theta_2, \theta_3, \theta_4) = \sqrt{\frac{k\sqrt{k_1^2 + k_2^2}}{\pi^3 k_2}} e^{ik_1 x_1} \left\{ \begin{matrix} \cos(k_2 x_2) \\ -i \sin(k_2 x_2) \end{matrix} \right\} J_{|m_2|}(k_3 r) \frac{e^{im_2 \theta_4}}{\sqrt{2\pi}}, \tag{6.23}$$

where  $k_1^2 + k_2^2 + k_3^2 = k^2$ .

(7) Polyspherical to double cylindrical coordinates in Fig. 7(14) ( $R \rightarrow \infty, J \sim kR, l_1 \sim k_3R, l_2 \sim k_1R$ ),

$$\begin{aligned} \lim_{R \rightarrow \infty} \frac{(-1)^{(J-l_2)/2}}{\sqrt{R}} \Psi_{Jl_1 l_2 m}(\theta_1, \theta_2, \theta_3, \theta_4) \\ = \sqrt{\frac{2k_1 k \sqrt{k_1^2 + k_2^2}}{\pi^3 k_2 k_3}} J_{|m|}(k_1 r) e^{im_2 \theta_4} \left\{ \begin{matrix} \cos k_3 x_3 \cos k_4 x_4 \\ -i \sin k_3 x_3 \cos k_4 x_4 \\ -i \cos k_3 x_3 \sin k_4 x_4 \\ -\sin k_3 x_3 \sin k_4 x_4 \end{matrix} \right\}, \end{aligned} \tag{6.24}$$

where  $k_1^2 + k_2^2 + k_3^2 = k^2$ .

(8) Polyspherical to Cartesian coordinates in Fig. 7(15) ( $R \rightarrow \infty, J \sim kR, m \sim k_1R, l_2 \sim k_2R, l_1 \sim k_3R$ ),

$$\begin{aligned} \lim_{R \rightarrow \infty} (-1)^{(J-m)/2} \Psi_{Jl_1 l_2 m}(\theta_1, \theta_2, \theta_3, \theta_4) \\ = \sqrt{\frac{8k\sqrt{k_1^2 + k_2^2}\sqrt{k_1^2 + k_2^2 + k_3^2}}{\pi^4 k_2 k_3 k_4}} e^{ik_1 x_1} \\ \times \left\{ \begin{matrix} \cos k_2 x_2 \cos k_3 x_3 \cos k_4 x_4; & -i \sin k_2 x_2 \cos k_3 x_3 \cos k_4 x_4; \\ -i \cos k_2 x_2 \sin k_3 x_3 \cos k_4 x_4; & -\sin k_2 x_2 \sin k_3 x_3 \cos k_4 x_4; \\ -i \cos k_2 x_2 \cos k_3 x_3 \sin k_4 x_4; & -\sin k_2 x_2 \cos k_3 x_3 \sin k_4 x_4; \\ -\cos k_2 x_2 \sin k_3 x_3 \sin k_4 x_4; & -i \sin k_2 x_2 \sin k_3 x_3 \sin k_4 x_4; \end{matrix} \right\}, \end{aligned} \tag{6.25}$$

where  $k_1^2 + k_2^2 + k_3^2 + k_4^2 = k^2$ .

As a final example, let us consider the contraction  $O(8) \rightarrow E(7)$  for the coordinate systems of Fig. 3. The contraction of the  $O(8)$  basis to the  $E(7)$  one in this case is ( $R \rightarrow \infty, l_1 \sim kR, l_2 \sim k_2R, l_3 \sim k_1R$ ):

$$\begin{aligned} \lim_{R \rightarrow \infty} \frac{1}{R^2} \Psi_{l_1 l_2 l_3 l_4 l_5 l_6 l_7}(\theta_1, \theta_2, \theta_3, \theta_4, \theta_5, \theta_6, \theta_7) \\ = \frac{\sqrt{k_2 k_3}}{2\pi r_2} J_{|l_4|}(k_2 r_1) J_{|l_5+1|}(k_3 r_2) e^{ik_1 x_1} e^{il_4 \theta_4} Y_{l_5 l_6 l_7}(\theta_5, \theta_6, \theta_7). \end{aligned} \tag{6.26}$$

### VII. CONCLUSION

In our previous paper<sup>1</sup> we studied contractions of all (i.e., both) coordinate systems on  $S_2$  to all (four) coordinate systems on  $E_2$ . Here we have presented all possible contractions of subgroup type coordinate systems on  $S_n$  to subgroup type ones on  $E_n$  for  $n$  arbitrary. Moreover, we have developed a graphical formalism illustrating these contractions.

Contractions of ellipsoidal and paraboloidal coordinate systems will relate more "exotic" special functions amongst each other. For instance, Lamé polynomials and their generalizations will go into Mathieu functions, parabolic cylinder functions, spheroidal functions, etc. Work in this direction is in progress.

## ACKNOWLEDGMENTS

We thank Professor E. G. Kalnins, Professor W. Miller, Jr., and Professor V. M. Ter-Antonyan for their interest and helpful discussions. We also thank Ye. M. Hakobyan for her help in the preparation of the diagrams. Two of the authors (G.P. and P.W.) thank each others' institutions for hospitality during mutual visits that made the research leading to the present article possible.

The research of P.W. was partially supported by research grants from NSERC of Canada and FCAR du Québec, that of G.P. by the RFBI grant N98-01-00330.

- <sup>1</sup>A. A. Izmest'ev, G. S. Pogosyan, A. N. Sissakian, and P. Winternitz, "Contractions of Lie algebras and separation of variables," *J. Phys. A* **29**, 5940–5962 (1996).
- <sup>2</sup>A. A. Izmest'ev, G. S. Pogosyan, A. N. Sissakian, and P. Winternitz, "Contractions of Lie algebras and separation of variables. Two-dimensional hyperboloid," *Int. J. Mod. Phys. A* **12**, 53–61 (1997).
- <sup>3</sup>P. Winternitz and I. Fris, "Invariant expansions of relativistic amplitudes and subgroups of the proper Lorentz group," *Sov. J. Nucl. Phys.* **1**, 636–643 (1965); *Yad. Fiz.* **1**, 889–901 (1965).
- <sup>4</sup>P. Winternitz, I. Lukac, and Ya. A. Smorodinskii, "Quantum numbers in the little groups of the Poincaré group," *Sov. J. Nucl. Phys.* **7**, 139–145 (1968); *Yad. Fiz.* **7**, 192–201 (1968).
- <sup>5</sup>J. Patera and P. Winternitz, "A new basis for representations of the rotation group. Lamé and Heun polynomials," *J. Math. Phys.* **14**, 1130–1139 (1973).
- <sup>6</sup>W. Miller, Jr., J. Patera, and P. Winternitz, "Subgroups of Lie groups and separation of variables," *J. Math. Phys.* **22**, 251–260 (1991).
- <sup>7</sup>W. Miller, Jr., *Symmetry and Separation of Variables* (Addison-Wesley, Reading, MA, 1997).
- <sup>8</sup>E. G. Kalnins, *Separation of Variables for Riemannian Spaces of Constant Curvature* (Longman, Burnt Mill, 1986).
- <sup>9</sup>N. Ya. Vilenkin, "Polyspherical and orispherical functions," *Mat. Sb.* **68**, 432–443 (1965).
- <sup>10</sup>N. Ya. Vilenkin, *Special Functions and the Theory of Group Representations* (American Mathematical Society, Providence, RI, 1968).
- <sup>11</sup>N. Ya. Vilenkin, G. I. Kuznetsov, and Ya. A. Smorodinskii, "Eigenfunctions of the Laplace operator realizing representations of the groups  $U(2)$ ,  $SU(2)$ ,  $SO(3)$ ,  $U(3)$  and  $SU(3)$  and the symbolic method," *Sov. J. Nucl. Phys.* **2**, 645–655 (1965); *Yad. Fiz.* **2**, 906–917 (1965).
- <sup>12</sup>M. S. Kildyushov, "Hyperspherical functions of the "tree" type in the  $n$ -particle problem," *Sov. J. Nucl. Phys.* **15**, 113–123 (1972); *Yad. Fiz.* **15**, 197–208 (1972).
- <sup>13</sup>G. I. Kuznetsov, S. S. Moskalyuk, Yu. F. Smirnov, and V. P. Shelest, *A Graphical Theory of Representations of Orthogonal and Unitary Groups and its Physical Applications* (Naukova Dumka, Kiev, 1992) (in Russian).
- <sup>14</sup>E. İnönü and E. P. Wigner, "On the contraction of groups and their representations," *Proc. Natl. Acad. Sci. USA* **39**, 510–524 (1953).
- <sup>15</sup>E. J. Saletan, "Contraction of Lie groups," *J. Math. Phys.* **2**, 1–21 (1961).
- <sup>16</sup>R. Gilmore, *Lie Groups, Lie Algebras and Some of their Applications* (Wiley, New York, 1974).
- <sup>17</sup>R. V. Moody and J. Patera, "Discrete and continuous graded contractions of representations of Lie algebras," *J. Phys. A* **24**, 2227–2258 (1991).
- <sup>18</sup>X. Leng and J. Patera, "Graded contractions of representations of  $sl(n, C)$  with respect to the maximal parabolic subalgebras," *J. Phys. A* **27**, 1233–1250 (1987).
- <sup>19</sup>M. Couture, J. Patera, R. T. Sharp, and P. Winternitz, "Graded contractions of  $sl(3, C)$ ," *J. Math. Phys.* **32**, 2310–2318 (1991).
- <sup>20</sup>M. Ait Abdelmalek, X. Leng, J. Patera, and P. Winternitz, "Grading refinements in the contractions of Lie algebras and their invariants," *J. Phys. A* **29**, 7519–7543 (1996).
- <sup>21</sup>P. Winternitz, "Successive refinements of gradings and graded contractions of  $sl(3, C)$ ," *Int. J. Mod. Phys. A* **12**, 109–115 (1997).
- <sup>22</sup>J. Patera, G. Pogosyan, and P. Winternitz, "Graded contractions of the Lie algebra  $e(2,1)$ ," CRM-2484, 1997.
- <sup>23</sup>E. Weimar-Woods, "Contractions of Lie algebras: generalized İnönü–Wigner contractions versus graded contractions," *J. Math. Phys.* **36**, 4519–4548 (1995).
- <sup>24</sup>L. P. Eisenhart, "Separable systems of Stäckel," *Ann. Math.* **35**, 284–305 (1934).
- <sup>25</sup>D. A. Suprunenko and R. I. Tyshkevich, *Commutative Matrices* (Academic, New York, 1968).
- <sup>26</sup>J. Patera, P. Winternitz, and H. Zassenhaus, "Maximal Abelian subalgebras of real and complex symplectic Lie algebras," *J. Math. Phys.* **24**, 1973–1985 (1983).
- <sup>27</sup>M. A. del Olmo, M. A. Rodriguez, P. Winternitz, and H. Zassenhaus, "Maximal Abelian subalgebras of pseudounitary Lie algebras," *Linear Algebr. Appl.* **135**, 79–151 (1990).



- <sup>28</sup>V. Hussin, P. Winternitz, and H. Zassenhaus, "Maximal Abelian subalgebras of complex orthogonal Lie algebras," *Linear Algebr. Appl.* **141**, 183–220 (1990).
- <sup>29</sup>V. Hussin, P. Winternitz, and H. Zassenhaus, "Maximal Abelian subalgebras of pseudoorthogonal Lie algebras," *Linear Algebr. Appl.* **173**, 125–163 (1992).
- <sup>30</sup>E. G. Kalnins and P. Winternitz, "Maximal Abelian subalgebras of complex Euclidean Lie algebras," *Can. J. Phys.* **72**, 389–404 (1994).
- <sup>31</sup>Z. Thomova and P. Winternitz, "Maximal Abelian subgroups of the isometry and conformal groups of Euclidean and Minkowski spaces," *J. Phys. A* **31**, 1831–1859 (1998).
- <sup>32</sup>M. N. Olevskii, "Orthogonal systems in spaces of constant curvature in which the equation  $\Delta_2 u + \lambda u = 0$  allows a complete separation of variables," *Mat. Sb.* **27**, 379–426 (1950) (in Russian).
- <sup>33</sup>E. Kalnins, W. Miller, Jr., and P. Winternitz, "The group  $O(4)$ , separation of variables and the hydrogen atom," *SIAM (Soc. Ind. Appl. Math.) J. Appl. Math.* **30**, 630–664 (1976).
- <sup>34</sup>G. Bateman and A. Erdélyi, *Higher Transcendental Functions* (McGraw-Hill, New York, 1953).